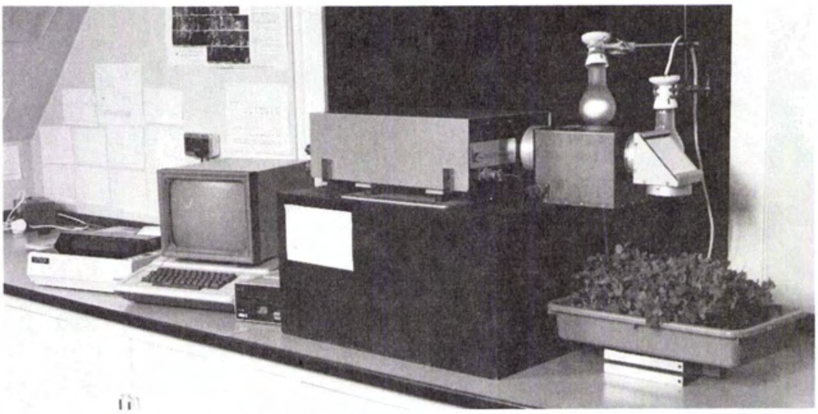

FRONTISPIECE. Prototype Barringer Refspec spectroradiometer.

D. C. FERNS*
S. J. ZARA
J. BARBER
Remote Sensing Group
Department of Pure and Applied Biology
Imperial College
London SW7 2BB, England

Application of High Resolution Spectroradiometry to Vegetation

A high resolution spectroradiometer is described which provides new information on vegetation canopy properties.

(Abstract on next page)

INTRODUCTION

PREVIOUS STUDIES of the spectral responses of vegetation have been largely of two types. First are those which use broad-band field spectroradiometers which typically have spectral bandwidths of 50 to 200 nm. Such instruments are of proven value both in relating spectral field measurements to satellite imagery, and in the use of broad-band infrared/red ratios which enhance the relationship between spectral and plant variables such as leaf area index and biomass (Kimes *et al.*, 1981).

A second type of study has used laboratory spectrophotometers yielding a spectral curve of high resolution, typically with bandwidths of 1 to 5 nm. Laboratory spectrophotometers have, however, many shortcomings which make it difficult to extrapolate their results to *in-situ* field measurements or remotely sensed imagery. These instruments are only able to measure a small area (2 cm^2) of a single leaf (or layered stack of leaves). Several canopy models (e.g., Allen and Richardson 1968; Smith and Oliver, 1972; Kimes *et al.*, 1979) have shown that the physiognomic structure of the plant canopy and light scattering between leaves causes the spectral response of a canopy to be notably different from that of single leaves. Furthermore, field reflectance measurements are greatly influenced by other factors such as solar zenith angle, azimuth angle, sensor look angle (Suits, 1972), and soil background reflectance (Curran, 1981).

Recent work has shown that additional information on vegetation is well correlated with wavebands not yet widely used, such as the middle infrared where reflectance increases with decreasing leaf water content (Ungar and Goward, 1982; Tucker, 1980). Additional information on vegetation is contained in narrow wavebands, and is only resolved with a sensor bandwidth of less than 4 nm (Collins, 1978; Horler *et al.*, 1981; Dockray, 1981). It is,

* Presently with Nigel Press Associates Ltd., Edenbridge, Kent TN8 6HS, United Kingdom.

0099-1112/84/5012-1725$02.25/0

ABSTRACT: *High resolution reflectance spectra of vegetation (with bandwidths of less than 5nm) contain information correlating to vegetation properties which is additional to the information content of broad spectral bands. A new term—the Leaf Overlap Index (LOI)—is introduced to explain a canopy property contributing to the shape of the "red edge" of the reflectance spectrum (680 to 750 nm). Studies of red edge features have been made using the prototype "Barringer Refspec" field spectroradiometer. This instrument has 934 wavebands, with a resolution of 1 to 3 nm between 460 and 2409 nm. An associated Apple II microcomputer allows spectra to be graphically displayed, stored, enlarged, printed, and digitally processed to produce smoothed, averaged difference or derivative spectra. Some initial results from this instrument are presented with particular reference to the principles of spectral interpretation in relation to species discrimination and vegetation stress detection. Also considered is the structure of the red edge, and the integration of high resolution data over broad bandwidths, for comparison with other radiometers.*

therefore, not difficult to surmise that an instrument, which produces high resolution spectra of hemispherical-directional reflectance measured in the field, may yield practical new information for applied remote sensing work. Before describing such an instrument, it is appropriate to review briefly some of the concepts on which high resolution spectroradiometry is based.

One major feature of vegetation spectra is the steep slope between the low visible reflectance and the higher near-infrared reflectance, commonly named the "red edge." When the visible-infrared reflectance spectrum of vegetation is displayed, the red edge often appears to be a featureless slope, and because the output of many spectrophotometers is greatly smoothed to "improve" the signal-to-noise ratio, the red edge has, until recently, not been subjected to detailed study. However, the first derivative curve of red edge reflectance displays troughs which correspond to changes in slope along the red edge, the deepest derivitive trough defining the wavelength of maximum slope of the red edge. An example of the red edge spectrum and its first derivitive, recorded using a Perkin Elmer 554 spectrophotometer, is shown in Figure 1.

Dockray (1981) and Horler *et al.* (1983) have shown that these "shoulders" in the red edge reflectance spectra, located by their corresponding troughs in the derivative spectra, bear some unique features which correlate well to the chlorophyll content of vegetation. On the limited evidence available, the red edge appears to have the following characteristics:

- With a decrease in chlorophyll content, the position of maximum slope of the red edge shifts to shorter wavelengths. Collins (1978) observed shifts of 7 to 10 nm during the growth and maturation of a wheat canopy. Shifts of 20 to 30 nm were observed in several species with increasing chlorophyll content per unit area of leaf (Dockray, 1981).
- A shift in the position of the maximum slope of the red edge of 18 nm was observed between four small areas along a single maize leaf, due to the fact that chlorophyll concentration naturally increases towards the older tissue at the leaf tip (Dockray, 1981).
- On correlating chlorophyll content against the position of the maximum slope of the red edge for the leaves of four cereal and four tree species, Dockray (1981) found r^2 values between 0.55 and 0.90, all significant at the 99.9 percent level.
- Although the maximum slope of the red edge shifted to longer wavelengths with an increasing number of stacked leaves, it did not appear to shift with the amount of leaf cover relative to bare ground (unlike broad-band red and near-infrared reflectance). Shifts of up to 27 nm were observed by stacking seven maize leaves.
- The derivative spectra enhances the detail of the red edge. Dockray found two derivative troughs, a shorter wavelength component, 'x', and a longer wavelength component 'y'. Component x was always present, and was dominant in single leaf reflectance measurements, but as leaves were stacked, the second component (y) gradually became dominant. Similarly, component x was dom-

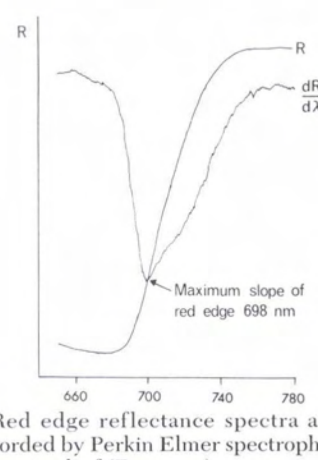

FIG. 1. Red edge reflectance spectra and derivitive spectra recorded by Perkin Elmer spectrophotometer. Example is a maize leaf (*Zea mays*).

inant in a sample of maize leaf from the stem junction, with component *y* increasing in dominance with samples from nearer the leaf tip, where higher chlorophyll concentrations were present. As a result of these component shifts, the position of the maximum slope of the red edge shifts to longer wavelengths as leaves are stacked or as chlorophyll content is increased. The shorter wavelength component *(x)* appears to relate directly to chlorophyll concentration in the leaf, while the origin of the longer wavelength component *(y)* remains unknown, but possible explanations based on the consideration of scattering have been put forward by Horler *et al.* (1983).

These results indicate that there are at least two factors which are related to the position of maximum slope of the red edge of relectance of a vegetation canopy: (1) chlorophyll concentration in the leaf, and (2) the degree of overlap between leaves.

It should also be noted that the above results indicate that the proportion of ground exposed to the sensor to that covered by leaves appears to have little or no effect on the position of the maximum slope of the red edge.

The Leaf Overlap Index (LOI)

In this paper we introduce a new term which quantitatively describes the degree of overlap of leaves within a vegetation canopy. This is the Leaf Overlap Index(LOI), defined as

$$\text{LOI} = \frac{\text{Projected Leaf Area*}}{\text{Projected Cover}}$$

$$= \frac{\text{Leaf Area Index**}}{\text{Percent Cover}} \times 100$$

* Along line of sight of sensor

** When sensor is nadir looking,

$$\text{and LAI} = \frac{\text{Total Leaf Area}}{\text{Ground Area}}$$

The application of the Leaf Overlap Index to the discrimination of different vegetation canopies is best described relative to Leaf Area Index (LAI) with reference to Figure 2.

LOI is an improvement on LAI in discriminating nine type-pairs of figure 2:

B from C, E, and F;
C from E, F, and G;
E from F and G; and
F from G.

LAI remains better than LOI in discriminating five of the type-pairs in Figure 2:

A from B, E, F, and G; and
C from D.

The two indices are therefore complementary in extracting useful information from vegetation canopies.

Leaf Area Index is defined irrespective of the remote sensor look angle, but the Leaf Overlap Index is a function of the sensor look angle. This is well illustrated by comparing Figures 2c and 2f, which show the same diagrammatic canopy structure orientated at different angles. This reorientation has the same effect as changing the look angle of the sensor. LAI had the same value for both orientations, but the LOI changes dramatically from 3 when the canopy has a horizontal structure (planophile) to 0 when reorientated to the vertical (erectophile) plane. However, most radiometers are used in a nadir-looking mode, and in such instances the Leaf Overlap Index can be defined using the easily measured percent cover and Leaf Area Index. LOI will be a good discriminator of the height of planophile canopies, and will also be a good discriminator between planophile canopies (with dominant horizontal leaf components) and erectophile canopies (with dominant vertical leaf components). Any change in leaf orientation in the canopy, such as wilting due to water stress, should be easily discriminated. To detect a change in leaf chlorophyll content by a shift in the maximum slope of the red edge over a vegetation canopy, it is envisaged that comparison would be needed to a "control" canopy of the same species and Leaf Overlap Index which had different leaf chlorophyll concentrations. The wavelength of maximum slope of the red edge reflectance cannot therefore be causally related to either LAI or percent cover without *a priori* knowledge of one of these variables. The use of LOI as a vegetation canopy property directly related to the wavelength of maximum slope of the red edge will help our understanding of how environmental variables such as metal toxicity cause the red edge slope to change.

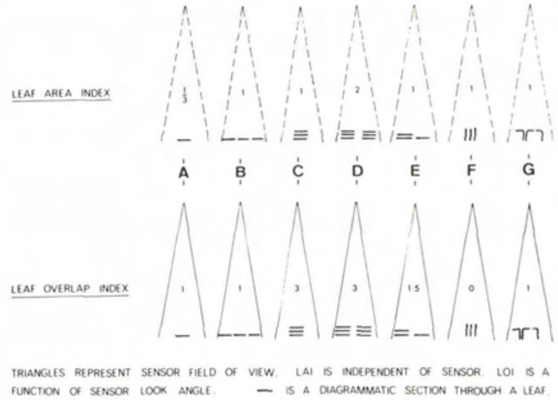

FIG. 2. Diagrammatic comparison of Leaf Area Index (LAI) and Leaf Overlap Index (LOI).

TABLE 1. REFSPEC WAVEBAND CHARACTERISTICS

Grating Order	Filter	Detector	Wavelength (nm)	Waveband number	Resolution (nm)
1	1	PbS	2409-1693	1-239	3.0
1	2	PbS	1693-1025	240-460	3.0
2	3	PbS	1004-0688	461-670	1.5
3	4	Silicon Diode	0725-0591	671-803	1.0
3	5	Silicon Diode	0591-0460	804-934	1.0

The authors are currently working on the application of these findings with a high resolution field spectroradiometer which measures the hemispherical-directional reflectance of a vegetation canopy. This spectroradiometer is the prototype "Barringer Refspec," illustrated in the frontispiece.

DESCRIPTION OF THE "BARRINGER REFSPEC"

TECHNICAL DETAILS

Powered by a 12V portable shoulder-pack battery, the Refspec combines the attributes of both filter wheel and grating mechanisms. Five filters in a single "wheel" are synchronized with a scanning monochromator (grating) mechanism, which completes three traverses in one spectral scan. This arrangement covers the spectral range from 460 to 2400 nm with a resolution of 1 nm in the visible, 1.5 nm in the near infrared, and 3 nm in the middle infrared wavelengths (see Table 1)—a total of 934 discrete wavebands.

The full scan, in five segments, is completed in 60 seconds. The instrument can have either an analog chart recorder output or digital cassette tape output by means of a PCD Digideck P71 data logger. The field of view of the instrument is a rectangular 12° by 6°. The arrangement of the equipment in the laboratory, illustrated in the frontispiece, was such that the canopy sample size integrated in the instantaneous field of view (IFOV) of the Refspec was approximately 8 cm by 4 cm. Positioning the sensor head above the canopy was done with great care to ensure that canopy morphology and cover were the same for each experimental sequence. The plant material chosen—pea seedlings (*Pisum sativum*)—was densely planted, so that in each experiment the IFOV contained a representative sample of the entire canopy. When a sensor is raised higher above the a canopy, there is no guarantee that the recorded reflectance of that canopy will not change, due to the interactions of several factors including the solar azimuth and zenith angles, atmospheric transmission, and the degree of horizontal homogeneity of canopy structure (Daughtry *et al.*, 1981; Jackson *et al.*, 1979; 1980). Nevertheless, the authors consider that close-range canopy measurements from the Refspec in the laboratory are considerably easier to extrapolate to airborne and satellite sensors than single leaf spectrophotometer measurements. The Refspec signal recorded by the output device is "hemispherical-directional" reflectance, as defined by Duggin (1980). This represents hemispherical or global irradiance, received by the $BaSO_4$ integrating sphere (a cosine receptor) divided by the reflectance of the target as seen through the 12° by 6° field of view. Depressed in the top of the instrument is a white sphere, coated on the interior surface with barium sulphate ($BaSO_4$), used as a standard reference material. Toward the base of the sphere are two slits through which light passes from the target and chopper wheel on one side, to the grating monochromator, filter wheel, and detectors on the other. The chopper wheel controls precisely what is measured at any one instant. It has six sectors, which are two "sets" of

(a) white $BaSO_4$,
(b) matt black (absolute reflectance properties shown in Table 2), and
(c) an aperture which allows light to be received from the target.

Thus, the following relationships apply: a-b is proportional to the intensity of diffuse or direct radiation and c-b is proportional to the intensity of radiation reflected from the target. The a-b signal is fed back to a variable gain control (G) which relates the signal to a constant battery reference voltage. The same gain is applied to a, b, and c.

The Refspec signal output is, therefore:

$$G\frac{(c - b)}{(a - b)};\ \text{i.e., } G\frac{(\text{TARGET} - \text{BLACK})}{(\text{BaSO}_4 - \text{BLACK})} = \frac{\text{TARGET}}{\text{BaSO}_4} = \text{HEMISPHERICAL-DIRECTIONAL REFLECTANCE}$$

THE APPLE II MICROCOMPUTER LINK

The Refspec is in use in the laboratory during the winter months, where it is connected to an Apple II microcomputer with a peripheral dot matrix printer and graphics tablet. The analog output from the Refspec is passed through an analog to digital converter (CCS 7470) in the Apple II. In-house soft-

TABLE 2. ABSOLUTE REFLECTANCE PROPERTIES OF MATT BLACK PAINT USED AS ZERO REFERENCE ON REFSPEC CHOPPER WHEEL

Wavelength (micrometres)	Reflectance (percentage)
0.4	3
1.2	3
1.4	4
1.6	5.5
1.8	5.5
2.0	7.5
2.2	9
2.4	11

ware has been developed to display a graphical output of a spectra on the VDU screen. However, the Refspec outputs 934 discrete wavebands, relative to only 240 display points used on the Apple screen. Therefore, a full spectral scan can only be displayed at reduced resolution—approximately every third band. To overcome this problem, software allows the user to display any portion of the spectrum at full resolution, with a defined wavelength scale at intervals of 2 to 6 nm. The red edge, for example, may be enlarged, displaying the 100-nm wavelength range from 650 nm to 800 nm across the full screen. A derivative program may also be called upon, and the result can be overlain on the red edge slope (Figure 3).

Spectra may be smoothed to reduce random noise using a running average function, which can be passed over the data any number of times. Five passes is usually sufficient, but it helps to experiment interactively depending on the original scatter of data. Spectra may be saved on floppy disk and recalled to be overlain by other spectra on the display screen, and the mean and variance of several spectra may be compared and displayed. Any display on the Apple screen can be printed out on a matrix printer within about 40 seconds. To conserve storage space on floppy disks, spectral data can be saved on permanent magnetic tape files by means of a link between the Apple and Imperial College Computer Centre. The graphics tablet can be used for several functions such as annotation of the display screen and measuring the area under a spectral curve.

When the Refspec is used in the field, spectra data are recorded in two-track binary code onto cassette tape by the PCD P71 data logger. An interface has been developed to make this cassette tape compatible with the Apple II system, where the tapes are read in using an audio tape recorder.

CONTROL TESTS OF THE SIGNAL-TO-NOISE RATIO

One of the most important aspects of high resolution spectroradiometry is the optimization of the signal-to-noise ratio. Collins *et al.* (1980) found that environment-induced noise in field spectra was generally two orders of magnitude greater than the subtle features associated with vegetation stress. This noise is to a large extent scattered energy which is a constant for any wavelength, and therefore frequency information of less reflective magnitude than this scatter may be extracted from the data only if both the signal-to-noise ratio and waveform smoothing functions are optimized. Vanderbilt (1981) implies that slight adjustment of the ratio can confuse whether or not a feature of the waveform is "real" (i.e., caused by the physical or biological characteristics of the target reflectance) or simply "noise."

Noise which occurred at the four filter wheel/grating changes has been successfully eliminated by software related to a voltage signal from the Refspec which recognizes the breaks in scanning. The signal-to-noise ratio was optimized in laboratory conditions by changing the position and intensity of the light source.

Averaging several spectra of the same target produced only a small further reduction in noise, suggesting that the major component of the noise was systematic. The use of a running average smoothing function removed this noise more effectively. The smoothing function was applied repeatedly until the form of the spectral curve stabilized. Figure 4 illustrates the noise reduction achieved with two, five, and ten applications of the smoothing function.

Experience has shown that real features of the

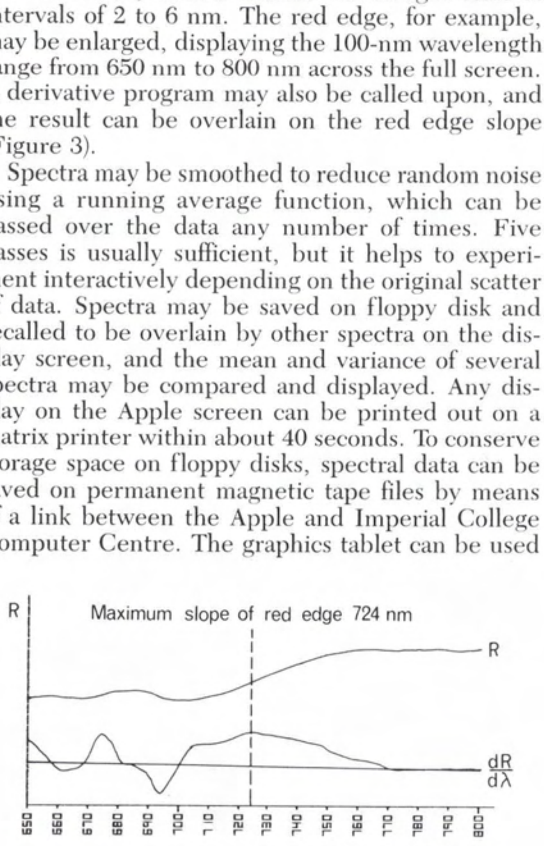

FIG. 3. Red edge reflectance spectra and derivative spectra recorded by Refspec radiometer. Example is a pea canopy (*Pisum sativum*).

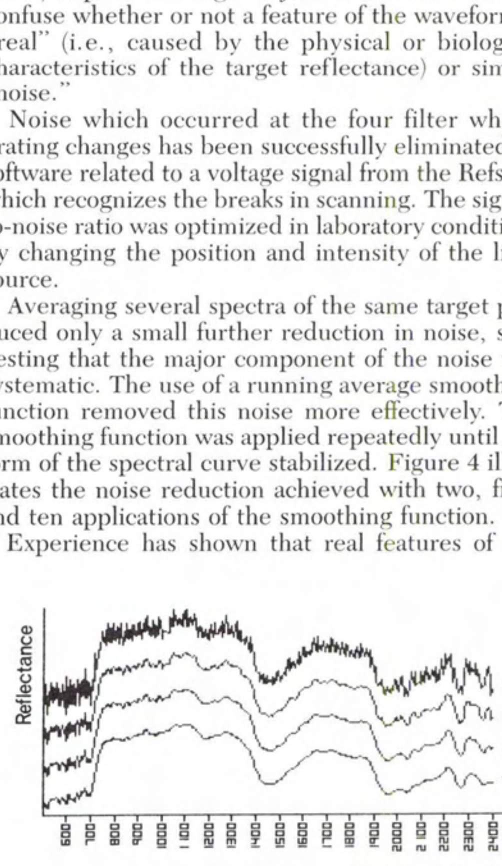

FIG. 4. Noise reduction achieved with two, five, and ten passes of a smoothing function.

waveform can only be defined when they have occurred at precisely the same wavelength (within 2 nm) on numerous occasions, with different samples, and preferably, different species.

Early Results

PRINCIPLES OF SPECTRAL DISCRIMINATION

A useful comparison can be made between the discrimination of clay mineral types and vegetation types. The principles of clay mineral discrimination by high resolution spectroradiometry, as outlined by Hunt and Ashley (1979), are very different from those of vegetation discrimination. Typically, different clay minerals exhibit spectra with troughs and peaks at significantly different wavelengths, due largely to the manner in which H_2O molecules are bound to the clay mineral structure. Thus, the presence or absence of troughs at these specified wavelengths defines the presence or absence of the mineral. Four clay mineral spectra recorded on the Refspec are shown in Figure 5.

However, the spectra of widely different types of vegetation can have extremely similar spectral responses. An example is shown by the similar spectra of a turf moss (*Fissidens taxifolius*) and of Scots Pine twigs (*Pinus sylvestris*) (Figure 6). The wavelengths of reflectance peaks and troughs are defined by the spectral characteristics common to all types of green vegetation. Chlorophyll, the chief influence on visible reflectance, and leaf water content, the chief influence on middle infrared reflectance, are the two dominant constituents of green leaves, while both the cellular structure of the leaf and the density of leaf area influence the near-infrared reflectance. Such relationships cause vegetation reflectance to change throughout the year.

SPECIES DISCRIMINATION

In order to distinguish vegetation types, it is particularly useful to have reference to phenological-spectral curves to find the best separability in terms of the vegetation growth stage (phenology and age), and also the optimum waveband(s) to be used. Ungar and Collins (1977) compiled an "atlas" of high resolution spectra of selected crops, with details of soil type, crop development stage and height, tone and texture on aerial photography, etc. Further work of this type, particularly on forest species, grasslands, and upland vegetation, may prove to be of significant value for forest, ecological, and land-use mapping. High resolution spectra have been recorded in the past with the intention of cataloging unique target signatures of particular crops. Although it is now clear that the objective of this work was not met, the same high resolution spectra offer a useful basis for identifying the best phenological stages for discrimination between crop types. Considerably less spectral information is available for the identification of growth stages of natural and semi-natural vegetation.

VEGETATION STRESS

The spectral response of vegetation is also affected by the condition or health of the plants. Plant condition may be measured experimentally in degrees of stress against a control plant, or simply in relative degrees of stress, such as "p.p.m. of toxic metal in foliage." Low resolution imagery and spectroradiometry cannot currently distinguish between different types of vegetation stress.

Early Refspec results confirm the potential for the discrimination water stress using high resolution spectra in the middle infrared (Figure 7). The spec-

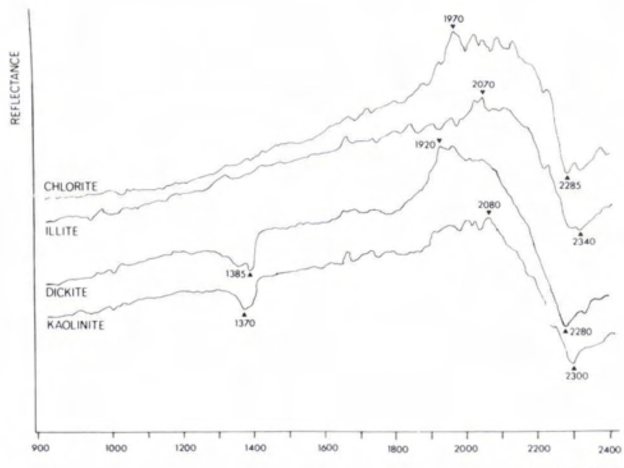

Fig. 5. Spectra of chlorite, kaolinite, illite, and dickite. All spectra drawn to some arbitrary reflectance scale, but with different baseline shifts to facilitiate shape comparisons.

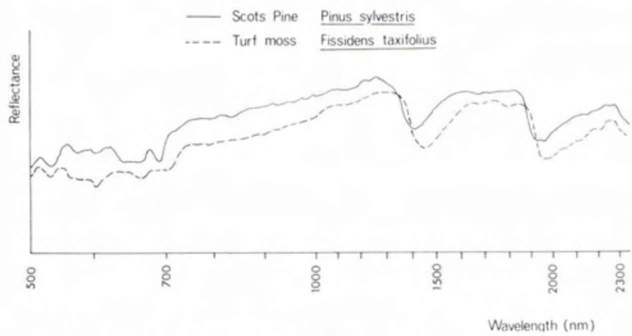

FIG. 6. Spectra of Scots Pine (*Pinus sylvestris*) needles and a turf moss (*Fissidens taxifolius*).

tral response of a water-stressed vegetation canopy confirms similar results from single-leaf spectrophotometer measurements (Hoffer and Johannsen, 1969).

A definitive spectral identification of water stress in vegetation with a minimum of ground information would, for example, have potential in (a) defining areas of excess drainage in agriculture, and (b) defining areas of water stress in forested areas, which are currently a major cause of commission errors in the identification of geobotanical anomalies for mineral and oil exploration.

The discrimination of water stress, however, may not be as simple as first appears. For example, it may be argued that metal toxicity stress causes physiological root damage to plants, and thus the roots are also less efficient in their uptake of water. Conversely, however, if the adaptation to metal stress increases the overall tolerance of the plant, then the metal-stressed plant may also be more tolerant of water stress. It may be expected that such relationships are variable between species.

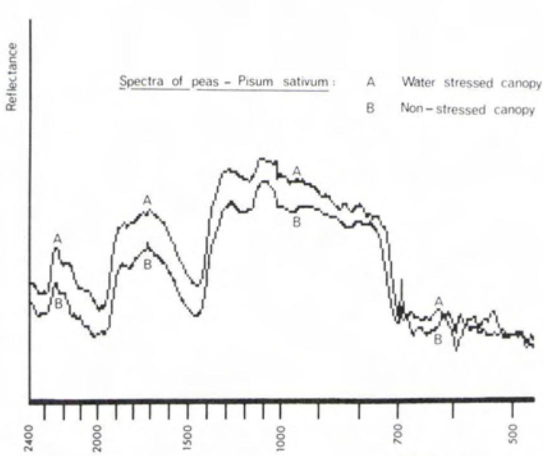

FIG. 7. Spectra of healthy and water stressed pea canopy (*Pisum sativum*).

RED EDGE STRUCTURE

The fine structure of the red edge is being studied in a series of ongoing experiments. Typically, ten separately recorded spectra, which have each undergone five passes of the smoothing function described above, are statistically analyzed to obtain the mean spectrum and its confidence limits. The differential curves are obtained from the smoothed, averaged red edge curves, and are similarly processed. Although averaging did not remove much of the noise, it successfully reduced the reflectance variations between different spectra.

To further investigate the effects of leak stacking, cucumber (*Cucurbita pepo*) plants were placed below the Refspec sensor over a background of dry soil and were arranged to present LOIs of 1,2,3,4, and 5 to the sensor. The resulting spectra, and the corresponding derivative spectra, are shown in Figures 8a to 8e. The derivative spectra locate the changes of gradient of the red edge, showing that there is a shift in the position of maximum red edge gradient towards longer wavelengths with increasing LOI, and the differential remains near its maximum value over an increasing wavelength range with increasing LOI, always returning to zero (marking the end of the red edge) at 755 to 760 nm.

The differential appears to contain components at 705 to 710 nm and 725 to 730 nm, the position of maximum slope being determined by the relative intensities of these two components. This closely resembles the results obtained by Dockray (1981) and Horler *et al.* (1983), described above.

A comparison of the derivative spectra of the red edge of peas (Figure 3) and cucumbers (Figures 8a to 8e) shows distinct differences in the wavelength-slope relationships. Further work will explore the possibilities of classifying derivative spectra as an aid to species discrimination.

BROAD-BAND INTEGRATION AND INSTRUMENT COMPARISONS

The high resolution output of the Refspec may be used to define the best broad spectral bands (e.g.,

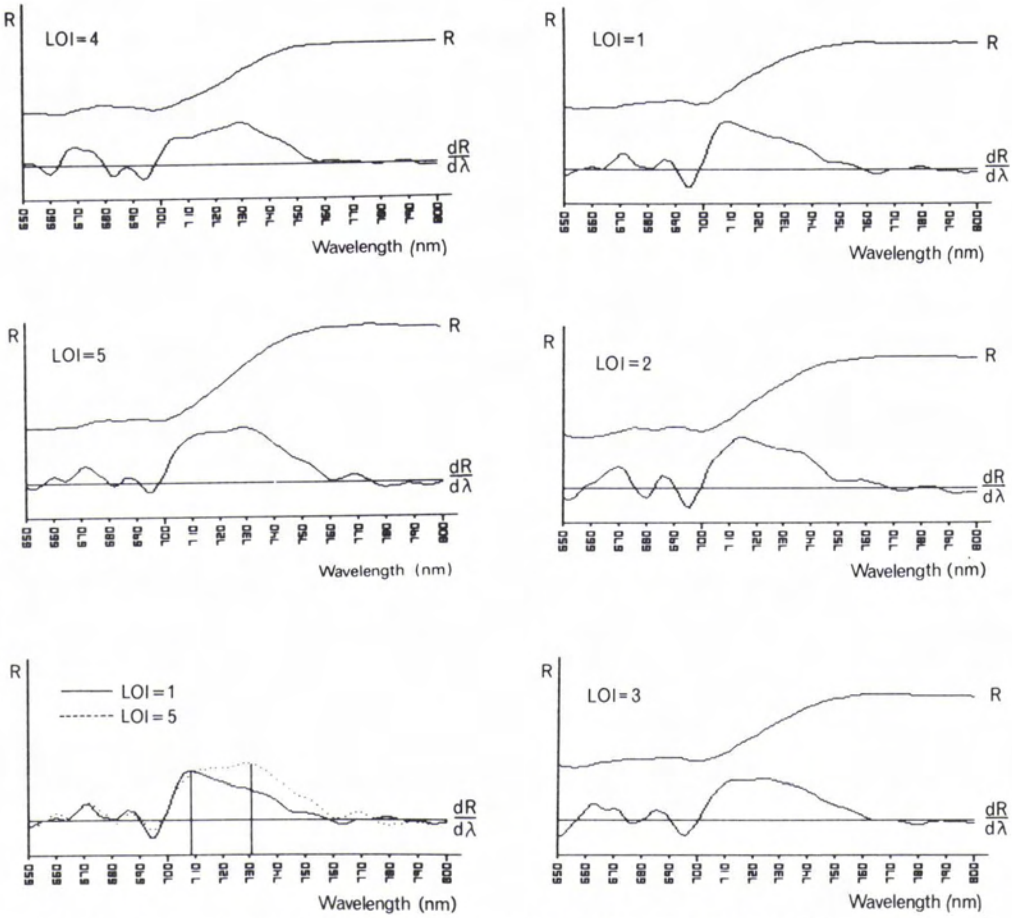

FIG. 8. (a to e) Red edge spectra and derivitives of cucumber (*cucurbita pepo*) leaves, with a LOI of 1 to 5, respectively; (f) The shift in the derivitive peak from 708 nm at LOI = 1 to 732 nm at LOI = 5.

20 to 100 nm) to discriminate any targets of interest. With carefully chosen waveband filters, a simple two-band radiometer may, for example, be as useful as the 934-band Refspec. A brown earth soil (from Sutton Bonington, Nottinghamshire) in four soil surface states (wet clod, dry clod, wet panned, dry panned) was measured using both the Barringer Refspec and broad-band Milton radiometer. The Milton radiometer was used in "Landsat MSS" wavebands 5 and 7 (600 to 700 and 800 to 1100 nm, respectively), and bidirectional reflectance was measured relative to a Kodak 18 percent grey card (Milton, 1981). Spectra of the same soil surfaces and the grey reference card were output from the Refspec, and the nearest equivalent measure to the Milton bands was calculated. This was done by measuring the area under the spectral curves using the Apple graphics tablet, between wavelengths 600 to 700 and 800 to 1100 nm, and dividing the area under the target curve by the respective area under the grey card curve. As expected, when the band 7 results are plotted against band 5, the four points representing the four soil surface states lie on a straight line, namely, the "soil background line" as defined by Richardson and Weigand (1979). However, the absolute values of bidirectional reflectance differed between the Milton and integrated Refspec data, resulting in a soil background line of a different slope (Figure 9). This type of study may be used to determine the instrument calibration factors. The differences between the relative spectral response functions of the Milton sensors and the integrated Refspec response are the most likely cause of the discrepancy between the two soil background lines (Figure 9), but other effects, such as instrument field of view, cannot be dismissed. When a broadband sensor has a non-uniform response over its spectral range, reflectance readings obtained from the sensor will not be the same as readings obtained from a high-resolution sensor integrated over the

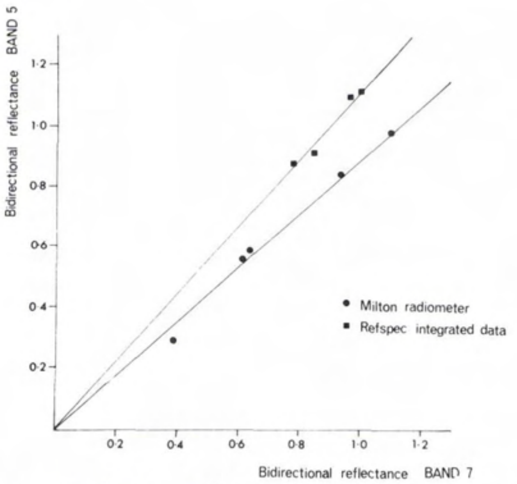

FIG. 9. Soil background lines as derived from Refspec and Milton radiometers.

same spectral range. This can be demonstrated as follows:

Let Rt(1), Rt(2), Rt(3), . . . , Rt(n) be the radiance values from a target over n adjacent wavebands (resolved by a high-resolution sensor).

Let Rr(1), Rr(2), Rr(3), . . . , Rr(n) be the radiance values from the reference surface at the above wavebands.

Let Fh(1), Fh(2), Fh(3), . . . , Fh(n) be the response functions of the high-resolution sensor at the above wavebands—these will be simply multiplication factors if there is no "dark current," i.e., the reading from the sensor is zero when intercepting zero radiance.

Let Fb(1), Fb(2), Fb(3), . . . , Fb(n) be the response functions of the broad-band sensor at the above wavebands.

The reflectance value from the high-resolution sensor integrated over the n wavebands is given by

$$\frac{\mathrm{Fh}(1)\mathrm{Rt}(1)}{\mathrm{Fh}(1)\mathrm{Rr}(1)} + \frac{\mathrm{Fh}(2)\mathrm{Rt}(2)}{\mathrm{Fh}(2)\mathrm{Rr}(2)} + \frac{\mathrm{Fh}(3)\mathrm{Rt}(3)}{\mathrm{Fh}(3)\mathrm{Rr}(3)} + \ldots + \frac{\mathrm{Fh}(n)\mathrm{Rt}(n)}{\mathrm{Fh}(n)\mathrm{Rr}(n)}$$

which simplifies to

$$\frac{\mathrm{Rt}(1)}{\mathrm{Rr}(1)} + \frac{\mathrm{Rt}(2)}{\mathrm{Rr}(2)} + \frac{\mathrm{Rt}(3)}{\mathrm{Rr}(3)} + \ldots + \frac{\mathrm{Rt}(n)}{\mathrm{Rr}(n)}$$

The reflectance reading from the broad-band sensor is given by

$$\frac{\{\mathrm{Fb}(1)\mathrm{Rt}(1) + \mathrm{Fb}(2)\mathrm{Rt}(2) + \mathrm{Fb}(3)\mathrm{Rt}(3) + \ldots + \mathrm{Fb}(n)\mathrm{Rt}(n)\}}{\{\mathrm{Fb}(1)\mathrm{Rr}(1) + \mathrm{Fb}(2)\mathrm{Rr}(2) + \mathrm{Fb}(3)\mathrm{Rr}(3) + \ldots + \mathrm{Fb}(n)\mathrm{Rr}(n)\}}$$

which cannot be further simplified.

It is, therefore, clear that integrated narrow wavebands recorded on high-resolution spectroradiometers may not be expected to correspond to results of broad-band radiometers without both an understanding of the instrument differences and the application of appropriate correction functions.

CONCLUSIONS

High resolution spectroradiometry is a relatively new tool in remote sensing, and is likely to see rapid development in the next decade. It is not only useful in defining the best wavebands for remotely sensed imagery; direct spectral results from ground and airborne spectroradiometers have already proved their commercial value in mineral exploration. The Collins airborne spectroradiometer (developed from that described by Chiu and Collins (1978)) has recently detected several mineral exploration targets; (Birnie and Francica, 1981; Collins, 1982; Collins *et al.*, 1980a, 1980b, 1982a, 1982b; McKeon and Marsh, 1982; Podwysocki *et al.*, 1982) chiefly by analyzing the red edge shift over biogeochemical anomalies. Instruments such as the Refspec fulfill the neglected role of understanding and interpreting high resolution vegetation reflectance spectra, to further the successful application of high resolution spectroradiometry in mineral exploration, species mapping, and stress type discrimination.

ACKNOWLEDGMENTS

The work has been funded by the Natural Environment Research Council (N.E.R.C.). D. C. Ferns and S. J. Zara were both in receipt of N.E.R.C. studentships. The authors thank M. Dover and J. De Felice for technical assistance, and Suzanne Cheston for typing the manuscript.

REFERENCES

Allen, W. A., and A. J. Richardson 1968. Interaction of light with a plant canopy. *Journal of the Optical Society of America* 58:1023-1028.

Annon, 1982. *Barringer Refspec Operators Manual*. Barringer Research Ltd., Toronto, Canada.

Barber, J., and D. N. H. Horler, 1981. *Fundamental relationship between plant spectra and geobotanical stress phenomena:* final report on NASA contract NAS-5-23738, Oct. 1981, 63 p.

Birnie, R. W., and J. R. Francica, 1981. Remote Detection of Geobotanical Anomalies related to Porphyry Copper Mineralization. *Economic Geology* 76:637-674.

Chiu, H. Y., and W. Collins. 1978. A Spectroradiometer for Airborne Remote Sensing. *Photogrammetric Engineering and Remote Sensing* 44:507-517.

Collins, W., 1978. Remote Sensing of crop type and maturity. *Photogrammetric Engineering and Remote Sensing* 44:43-55.

———, 1982. The chlorophyll infrared edge shift and high spectral resolution techniques for mineral exploration. Presentation at "Remote Sensing for Exploration Geology" Fort Worth, Texas, 6-10 Dec. 1982 (2nd Thematic ERIM Conference).

Collins, W., S. H. Chang, and J. F. Koo, 1980. *Detection of hidden mineral deposits by airborne analysis of forest canopies*. University of Columbia, New York. NTIS Report PB80-19381.

Collins, W., S. H. Chang, J. F. Koo, and A. Mancinelli, 1980. *Biogeochemical laboratory studies to establish the spectral properties of mineral-induced stress in plants*. University of Columbia, New York. NTIS Report PB80-196769.

Collins, W., S. H. Chang, F. Canney, G. Raines and N. Milton, 1982. Application of the chlorophyll infrared edge shift in airborne exploration mapping of mineralized zones. Presentation at "Remote Sensing for Exploration Geology", Fort Worth, Texas. 6-10 Dec. 1982 (2nd Thematic ERIM Conference).

Collins, W., S. H. Chang, and G. Raines, 1982. Mineralogical mapping of Death Valley, Nevada, and Crossman Peak, Arizona, sites using airborne near infrared spectral reflectance. Presentation at "Remote Sensing for Exploration Geology" Fort Worth, Texas, 6-10 Dec. 1982 (2nd Thematic ERIM Conference).

Curran, P. J., 1981. Multispectral remote sensing for estimating biomass and productivity. In *Plants and the Daylight Spectrum*, ed. H. Smith, Academic Press, London.

Daughtry, C. S. T., V. C. Vanderbilt, and V. I. Pollara, 1981. *Variability of reflectance measurements with sensor altitude and canopy type*. N.A.S.A. Report Number NAS-9-15466.

Dockray, M., 1981. *Verification of a new method for determining chlorophyll concentration in plants by remote sensing*. Thesis for M.Sc. and DIC, 1981. Centre for Environmental Technology, Imperial College, University of London.

Duggin, M. J., 1980. The Field Measurement of Reflectance Factors. *Photogrammetric Engineering and Remote Sensing* 46:643-647.

Hoffer, R. M., and C. J. Johannsen, 1969. Ecological potentials in spectral signature analysis, In P. L. Johnson (ed.), *Remote Sensing in Ecology*, University of Georgia Press, Athens.

Horler, D. N. H., M. Dockray, and J. Barber, 1983. The red edge of plant leaf reflectance. *International Journal of Remote Sensing*, 4(2), 273-288.

Hunt, G. R., and R. P. Ashley, 1979. Spectra of altered rocks in the visible and near-IR. *Economic Geology* 74:1613-1629.

Jackson, R. D., P. J. Pinter, S. B. Idso, and R. J. Reginato, 1979. Wheat Spectral Reflectance: Interactions Between Crop Configuration, Sun Elevation and Azimuth Angle. *Appl. Optics*, 18(22), 3730-3731.

Jackson, R. D., P. J. Pinter, R. J. Reginato, and S. B. Idso, 1980. Hand-Held Radiometry. *SEA/AR Workshop*, Phoenix, Arizona, 25-26 February. U.S. Dept. of Agric. Rep. USDA/SEA-ARM-W-19 65 p.

Kimes, D. S., *et al.*, 1979. *Terrain feature canopy modelling*. Colorado State University Report, Fort Collins; College of Forestry, Apr. 1979, 225p.

Kimes, D. S., B. L. Markham, C. J. Tucker, and J. E. McMurtey, 1981. Temporal relationships between spectral response and agronomic variables of a corn canopy. *Remote Sensing of Environment* 11:401-411.

McKeon, J. B., and J. E. Marsh, 1982. Integrated analysis of high resolution field and airborne spectroradiometer data from an epithermal gold district. Presentation at "Remote Sensing for Exploration Geology", Fort Worth, Texas, Dec. 6-10, 1982 (2nd Thematic ERIM Conference).

Milton, E. J., 1980. A portable multiband radiometer for ground data collection in remote sensing. *International Journal of Remote Sensing* 1:153-66.

Podwysocki, M. H., D. B. Segal, W. Collins, and S. N. Chang, 1982. Mapping the distribution of hydrothermally altered rocks by using airborne multispectral scanner and spectroradiometer data. Marysvale, Utah. Presentation at "Remote Sensing for Exploration Geology", Fort Worth, Texas, 6-10, Dec. 1982 (2nd Thematic ERIM Conference).

Richardson, A. J., and C. L. Wiegand, 1977. Distinguishing vegetation from soil background information. *Photogrammetric Engineering and Remote Sensing* 43:1541-1552.

Smith, J. A., and R. E. Oliver, 1972. Plant canopy models for simulating composite scene spectroradiance in the 0.4—1.05nm region. *Proceedings of the 8th International Symposium on Remote Sensing of Environment*, pp. 1333-1343.

Suits, G. H., 1972. The calculation of the directional reflectance of a vegetation canopy. *Remote Sensing of Environment* 2:117-125.

Tucker, C. J., 1980. Remote sensing of leaf water content in the near-infrared. *Remote Sensing of Environment* 10:23-33.

Ungar, S. G., W. Collins, and J. Coiner, 1977. *Atlas of selected crop spectra, Imperial Valley, California*.

NASA Institute for Space Studies, G.S.F.C. Tech. Mem. TM-9743, June 1977, 220 p.

Ungar, S. G., and S. N. Goward, 1982. Enhanced crop discrimination using the mid-IR (1.55—1.75nm). Presentation at Workshop on Selection and Impact of Spectral Bands for Earth Resources Analysis from Space, COSPAR, Ottawa, 31 May-2 June 1982.

Vanderbilt, V. C., E. R. Stoner, L. L. Biehl, B. F. Robinson, R. A. Weismiller, and M. E. Bauer, 1980. Fine structure in the spectral reflectance of vegetation and soils. *6th Ann. Symp. on Mach. Proc. of Remotely Sensed Data and Soil Information Systems and Remote Sensing and Soil Survey*, LARS, Purdue Univ., 3-6 June 1980.

(Received 22 July 1982; revised and accepted 18 June 1984)

SHORT COURSE

George Washington University Continuing Engineering Education

Washington, D.C.

Remote Sensing for Global Resource Applications: Principles and Techniques (4-8 February 1985)

Participants will learn the principles and concepts fundamental to successful use of remote sensor data for resource applications. Emphasis is on the principles of digital information extraction and the analysis techniques used for specific resource applications in mineral and petroleum exploration and assessment, forest management, cartography, land-use analysis, hydrologic applications, and agricultural crop yield and damage analyses.

For further information please contact Ron Donais, (202) 676-8523 or toll-free (800) 424-9733.

SHORT COURSES

Colorado School of Mines

Golden, Colorado

5 March 1985—State Plane Coordinates for Surveying and Mapping
One-Day Executive Seminar for administrators, planners and government officials.

6-8 March 1985—State Plane Coordinates for Surveying and Mapping
Three-Day Technical Workshop for surveying and mapping professionals.

For further information please contact Mrs. Reed, (303) 273-3329.

Special Invitation

The Engineering Applications Committee of the ASP Remote Sensing Applications Division wish to hold a special session on *Remote Sensing Solutions to Engineering Problems in New Frontier Areas* at the 1986 Fall Technical Meeting in Anchorage, Alaska. The committee welcomes early proposals for papers on this topic.

For further information please contact

Dr. Geoff Tomlins
B.C. Research Council
3650 Westbrook Mall
Vancouver, B.C. V6S 2L2
Canada
Tele. (604) 224-4331